Experimental Analysis of Enhanced Heat Transfer and Pressure-Drop of Serrated Finned-Tube Bundles with different Fin Geometries

RENE HOFMANN , FRIEDRICH FRASZ, KARL PONWEISER
Institute of Thermodynamics and Energy Conversion
Vienna University of Technology
A-1060 Vienna, Getreidemarkt 9/E302
AUSTRIA

Abstract: Experimental investigations have been carried out for heat transfer and pressure drop at turbulent flow of combustion gases at transverse serrated finned-tubes in cross-flow. I- and U-shaped fin geometries were considered, where the geometrical constants for the fins, i.e. height, fin pitch, fin thickness, and fin width were varied. For the design of heat exchangers with transverse finned tubes in cross-flow, it is necessary to consider the advantage and disadvantage of geometrical factors, which influence heat transfer and pressure drop. By means of experimental results and equations from literature the correlations for the Nusselt number *Nu* and pressure drop coefficient ξ were developed and compared. Additionally, a performance evaluation criterion was carried out for the two different fin geometries.

Key-Words: heat transfer, pressure drop, serrated fin, performance evaluation criterion, finned-tube bundles, experimental setup, Lévêque-Analogy, turbulent flow

1 Introduction

The demand for reducing primary energy claims an improvement of the efficiency of heat-exchangers, which contributes to the reduction of the CO_2 - production. Finned tubes are applied to enhance heat transfer. The heat transfer coefficient α_0 at the air-side of air/water tube heat exchangers, e.g. steam boilers or heat recovery boilers, is lower than the heat transfer coefficient at the inside of the water tubes. There are many possibilities to improve heat transfer at the air-side. On the one hand, the heat-transferring surface could be enlarged by an arrangement of annularly fins or other elements. This increase of the total tube surface allows transferring more heat from hot gases, but the demand on smaller installation sizes requires smaller fin pitch with larger fin height. On the other hand, finned tubes with segmented fins show a somewhat higher turbulence than those with smooth fins, because the boundary layer has to be built up anew at each segment [8]. Staggered arrangement of the tubes in the bundle could also increase turbulences. A higher pressure drop is caused by resistances in the flow channel and turbulences. To optimize a finned-tube heat exchanger means also to minimize the pumping power. Experimental investigations of solid and serrated finned-tubes have been studied extensively by [2], [6], [7], [9], [10] and [11]. Taborek [1] and Frasz [6] compared the different influences of solid and segmented fins, where Weierman [3] investigated the performance of in-line and staggered tube arrangement of segmented fin-tubes. Numerous correlations for the prediction of heat transfer of serrated fin tubes have been done by [5], [7] and [15], whereby Nir´s [5] correlations are based on numerous heat transfer and pressure drop data. Kawaguchi [7] specifies an accuracy of ±5 % for the equations, to predict the Nusselt number and the friction factor. Weierman´s [2] correlations for heat transfer at staggered layout show an expected accuracy of ±10 %; and for the pressure drop equations an accuracy of ±15 % is achieved. Heat transfer and pressure drop equations are functions of the geometrical parameters e.g. fin height, fin pitch, fin thickness, fin width, fluid properties, and variables of state, etc. To calculate the overall heat transfer of a finned-tube, according to the laws of heat conduction and heat convection, the fin efficiency, as a reduction coefficient has to be considered. Hashizume et al. [12] calculated the fin efficiency of serrated fins, using an analytical model with the assumption of a uniform heat transfer coefficient over the fin surface of the segmented section and a second equation for the theoretical fin efficiency. Kearney and Jacobi [4] investigated experimentally the local heat transfer behavior in staggered and in-line arrangement with the help of optical adaptation of the naphthalene sublimation technique, to evaluate the analytical fin efficiency. Webb [14] as well as Stephan and Mitrović [16] developed a criterion for the evaluation of the performance of a heat exchanger, to quantify the heat capacity by consideration of the pumping power. In

this study a performance evaluation of different finned-tubes in forced convection was analyzed. Especially the influence of the fin height was considered.

2 Experimental Setup

2.1 Test Facility

A test rig for heat transfer and pressure drop measurements at finned tube bundles in cross-flow is in operation at the laboratory of the Institute for Thermodynamics and Energy Conversion at the Vienna University of Technology. This test facility allows measuring at Reynolds numbers in the range between 4500 and 35000 and flue gas mass-flow from 0.6 to 4.5 kg/s; the layout is shown in figure 1. The finned-tube bundle is admitted with up to 400°C hot gas, which is generated by combustion of natural gas. Air intake is performed using a Venturi nozzle and a smaller ISA 1932 inlet nozzle for low *Re*-numbers, which are also used for mass flow measurement of combustion air. Following a connecting piece with a bend, a variable incidence entry vane is mounted in front of the radial fan for mass flow regulation of the air. The radial fan can produce a maximum pressure height of 5000 Pa and generates 45000 Nm³/h at 3500 Pa. The air flows through a three-meter conical connecting piece to the burner.

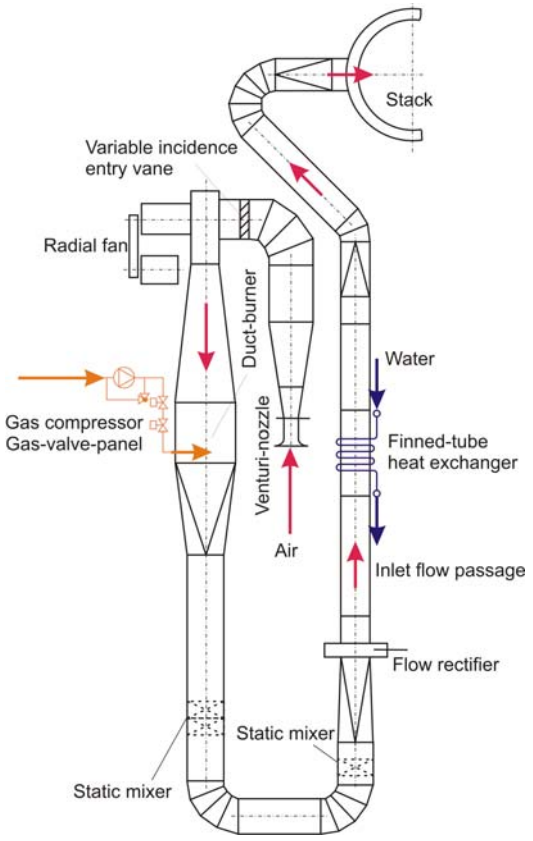

Fig.1: Layout and design of the test facility

The burner is designed as a duct burner, drawing its combustion air partly from the process air through ductings. The maximum burner power is 1160 kW.
Behind the burner, a tube follows with a diameter of 600 mm, in which a static mixer application is installed. After two 90° bends there is an additional mixer application, followed by a transition piece to a rectangular cross-section, 500 mm in width and 1000 mm in height, containing a flow rectifier, consisting of three fine wire meshes in close arrangement. After the flow rectifier, which rectifies the vortices caused by mixers and redirecting pipes, a 2000 mm inlet channel follows, which serves to calm the fully developed turbulent flow.
The finned tube heat exchanger with a tube length of approx. 500 mm is built into a 1500 mm channel piece. Behind this testing channel, the flue gas is conducted in a steel tube stack. The finned tube heat exchanger consists of a rectangular sheet steel channel in which the finned tubes are arranged horizontally with a given transverse and longitudinal pitch. The free channel width is fixed at 500 mm. All connecting pipes are arranged at the outside of the channel. This is the only arrangement allowing exact measurement of heat transfer at the small test section width of the tube banks. Measurements are thus not influenced by bypass flow through the space for the bends. The volume-flow of water is constant with V_W=14.1 m³/h at p_W=2.7 bar and a velocity of w_W=0.5 m/s. The tube bundle consists of 88 tubes, which are arranged in 8 consecutive columns, consisting of 11 horizontal tubes. An even cooling water flow distribution in the tubes is achieved by orifices after the inlet collector. The hot parts of the test facility are insulated using mineral wool, glass wool, and aluminum foil, to prevent heat loss. For more details see [8].

2.2 Measurement Procedure

The experimental investigation requires a number of measurements to be taken simultaneously in order to evaluate and determine the amount of transferred heat as well as gas-side pressure drop. A scheme of the measurement application is presented in figure 2. The temperatures on the water side are measured for every coiled tube at the inlet and at the outlet using Pt-100 RTDs (resistance temperature detectors), so that fringe effects can be ascertained for the outside tubes and considered in the evaluation. Gas temperatures are measured by NiCr-Ni thermocouples. To affect the flow pattern not significantly, the diameter of these thermocouples is chosen only 1.5 mm. Four thermocouples are arranged and mounted in front of and behind the heating surface of the heat exchanger, to obtain a grid measurement. 3 NiCr-Ni thermocouples

measure the air temperature at the Venturi nozzle and after the fan as well as the gas temperature after the burner. The mass flow of water is measured using a calibrated hot water meter with an electronic sensor.

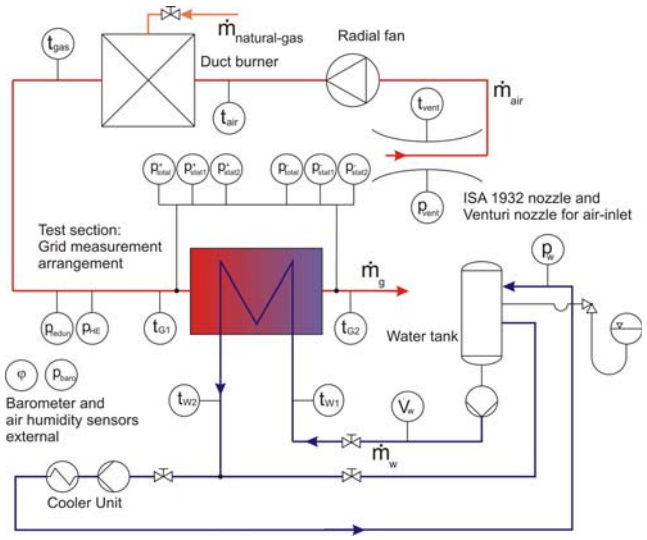

Fig.2: Measurement application

The mass flow of air is measured by determining the pressure difference at the Venturi nozzle in front of the inlet collector, using two different sensors: Honeywell Micro-switch series 160 (±0.25 % Full scale (FS)) and Furness Controls Micro-manometer (Meter scale ±19.99 mm H2O). The humidity of air is measured by means of an electronic humidity sensor. The barometric pressure is measured using Honeywell digital precision barometer HPB with an accuracy of ±0.4 hPa FS. The static pressure differences at the air-side of the finned-tube bundle are measured at four inlets in front of and behind the heating surface of the heat exchanger to obtain a grid measurement, using Honeywell digital precision pressure transducer PPT, with an accuracy of ±0.05 % FS. The total pressure differences in the center of the combustion-channel are measured using a United Sensor pitot-static-pressure probe. The absolute pressure in the combustion-channel is measured using Honeywell Micro-switch series 160 (±0.25 % FS). All measurement systems were pre-calibrated before application. The measured values are transmitted to the process computer with measurement value periphery by National Instruments and LabView 7.0E program system.

3 Test Geometries

Two finned tube geometries have been tested and analyzed, to characterize the influence on heat transfer and pressure drop for heat exchanger /geometry optimization. The test tubes with I- and U-shaped fin geometry are specified in table 1. For both tubes the transverse and the longitudinal pitch are equal.

Fin Geometry	I	U
Bare tube diameter	38.0 mm	38.0 mm
Tube thickness	4 mm	3.2 mm
Number of fins per m	276	295
Average fin height	15.5 mm	20.0 mm
Average fin thickness	1.0 mm	0.8 mm
Average tube length	500 mm	495 mm
Average segment width	4.5 mm	4.3 mm
Reduced fin height	16.7685 mm	21.5 mm
Number of tubes in the direction of the flow	8	8
Number of tubes per row	11	11
Longitudinal tube pitch	79 mm	79 mm
Transverse tube pitch	85 mm	85 mm
Total outside surface area of the bundle	64.047 m²	84.4815 m²
Fin material	St 37.2	DC01
Tube material	St 35.8	St 35.8
Net free area in a tube row	0.23269 m²	0.2292 m²

Table 1: Specifications of finned-tubes

The geometrical constant fin height varies most (I-fin 15.5 mm and U-fin 20 mm). The main advantages of the U-fin geometry (figure 3) are higher contact area between fin and tube (heat conduction) and smaller fin spacing possibilities, which would allow a higher total outside surface area of the bundle at equal or smaller installation size of the heat exchanger.

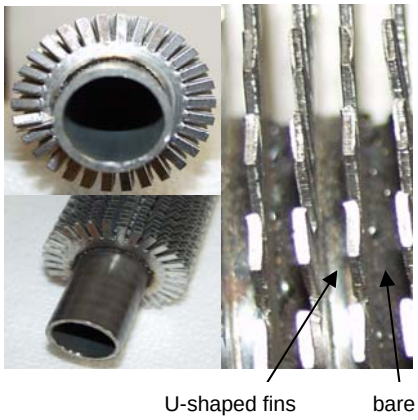

Fig.3: Experimental tube with U-fins

4 Data Reduction and Interpretation

4.1 Governing Heat Transfer Equations

The heat transfer rate of water is determined directly by

$$\dot{Q} = \dot{m}_w (h_{w_2} - h_{w_1}) . \quad (1)$$

The heat transfer rate of the combustion gas is defined by

$$\dot{Q} = \dot{m}_g c_{p_g} (T_{g_1} - T_{g_2}) . \quad (2)$$

Heat conduction through the tube wall is known as

$$\dot{Q} = kA_{tot}\Delta T_{ln}, \quad (3)$$

whereby k is the heat transfer coefficient of conduction, A_{tot} the total outside surface area of the bundle and the logarithmic mean temperature difference between input and output of the heat exchanger

$$\Delta T_{ln} = \frac{(T_{g_1} - T_{w_2}) - (T_{g_2} - T_{w_1})}{\ln \frac{T_{g_1} - T_{w_2}}{T_{g_2} - T_{w_1}}}. \quad (4)$$

For calculating the heat transfer of a finned tube, the convection and the heat conduction has to be considered. A reduction coefficient termed "fin efficiency" is therefore introduced, by which the actual heat transfer coefficient is multiplied in order to get the apparent heat transfer coefficient. The fin efficiency is calculated, according to the laws of heat conduction, under the assumption, that the actual heat transfer coefficient is uniformly distributed across the fin surface [8]. The apparent heat transfer coefficient is

$$\alpha = \frac{1}{\frac{1}{k} - f_a \frac{d_a}{d_i \alpha_i} - f_a \frac{d_a}{2\lambda_r} \ln \frac{d_a}{d_i}}. \quad (5)$$

With the help of the fin efficiency the actual (external) heat transfer coefficient at the surface is

$$\alpha_0 = \frac{\alpha A_{tot}}{A_{tube} + \eta_r A_{fin}}. \quad (6)$$

Then the dimensionless number Nu_0 with a characteristic dimension $l' = d_a$ at the medium gas temperature is calculated with

$$Nu_0 = \frac{\alpha_0 d_a}{\lambda_{gm}}. \quad (7)$$

By taking into account an average mean boundary-layer temperature

$$T_b = \frac{T_{wall} + T_{gm}}{2}, \quad (8)$$

the Nusselt number is defined as:

$$Nu_b = Nu_0 \frac{\lambda}{\lambda_b}. \quad (9)$$

4.2 Governing Pressure Drop Equations

The total pressure drop of the channel with inserts (tube bundle) is calculated with the following equation

$$\Delta p = N_R \xi \frac{\rho_{gm} w_E^2}{2}, \quad (10)$$

where ρ_{gm} and w_E are the arithmetic mean density and velocity in the net free area of a row, respectively.

$$w_E = \frac{\dot{m}_g}{F_{min}\rho_{gm}} \quad (11)$$

The pressure drop coefficients of the channel were correlated with the Konakov [17] equation

$$\xi_{ch} = \frac{1}{(1.8 \log Re - 1.5)^2}. \quad (12)$$

The properties for the physical quantities are based on the arithmetic mean temperature of hot gas between inlet and outlet. By considering the pressure variation as a result of the temperature change over the bundle, the pressure drop coefficient for the serrated tube bundle is calculated by

$$\xi_{8R} = \left(\Delta p - \left(\frac{\dot{m}_g}{A_{ch}} \right)^2 \left(\frac{1}{\rho_{g_1}} - \frac{1}{\rho_{g_2}} \right) \right) \frac{2}{\rho_{g_m} w_E^2} - 2\xi_{ch} \frac{L}{D_H}. \quad (13)$$

The average pressure drop coefficient for a single tube row is

$$\xi_{1R} = \frac{\xi_{8R}}{8}. \quad (14)$$

5 Comparison with Other Studies

5.1 Heat Transfer Correlations

The correlation of Escoa for external heat transfer at finned tubes with serrated fins in staggered arrangement of tubes is defined by

$$Nu = \frac{1}{4} Re^{0.65} Pr^{1/3} \left(\frac{T_{gm}}{T_s} \right)^{1/4} \left(\frac{d_a + 2h}{d_a} \right)^{1/2} C_3 C_5 \quad (15)$$

with

$$C_3 = \left(0.55 + 0.45 e^{\left(-0.35 \frac{h}{t-s} \right)} \right) \quad (16)$$

$$C_5 = \left(0.7 + \left(0.7 - 0.8 e^{-0.15 N_R^2} \right) \cdot e^{-\frac{t_l}{t_q}} \right). \quad (17)$$

For details see [15]. Figure 4 shows the dimensionless heat transfer coefficient for eight tube rows in staggered arrangement. The heat transfer coefficient of the I-fin tube is somewhat higher than that for the U-fin tube. Both, the U- and the I-fin-characteristic show app. same gradient. The exponents for the Nusselt correlations vary from 0.59 to 0.65. This variation could be caused by the uncertainty of the pressure difference measurement of the mass-flow of air at low Re-numbers. The measured results show good congruence with the equations of Escoa.

Since in (15)

$$Nu = f(Re, Pr, \vartheta_{gm}, \vartheta_s, d_a, h, t, s, t_q, t_l) \quad (18)$$

and the heat conduction through the tube and the fin is different for the two geometries, the formula for

the Nusselt number has to be converted for the same conditions.

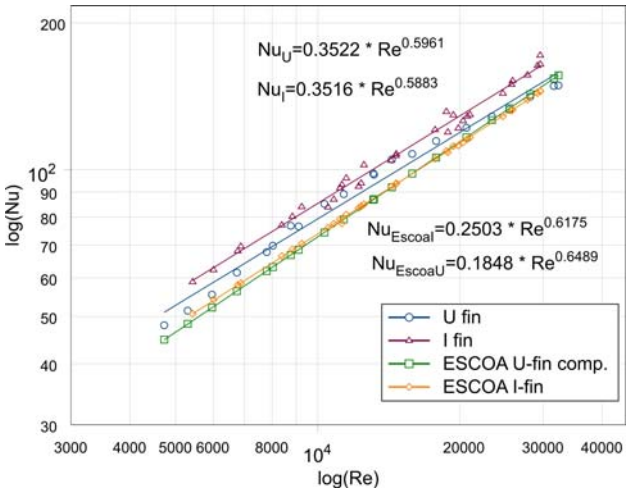

Fig.4: Heat transfer 8 tube rows, Pr=0.71, d=38 mm

C_5 does not change its value because of the same transverse and longitudinal pitch. Each point of the diagram is obtained at different temperatures. For further calculations a new average reference temperature for gas and fin has to be set. The Nusselt number changes then to

$$\mathrm{Nu_c} = \mathrm{Nu_U} \frac{\left(\frac{T_{gf}}{T_{sf}}\right)_I^{1/4}}{\left(\frac{T_{gm}}{T_s}\right)_U^{1/4}} \sqrt{\frac{d_a + 2h_I}{d_a + 2h_U}} \frac{C_{3I}}{C_{3U}}. \qquad (19)$$

If equation (19) is applied to the left side in (15), the factor h/(t-s) for U-fins calculates to 4.29 and for I-fins to 3.51. C_3 directly influences the heat transfer. If the exponent h/(t-s) in equation (16) lowers, C_3 increases and the overall heat transfer rises up to 6.5%.

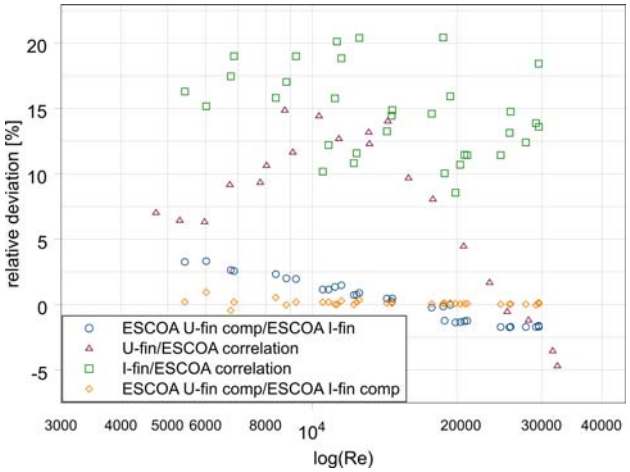

Fig.5: Relative deviation of correlations

Figure 5 shows the relative deviation of our measured values from the Escoa correlation for test geometries. The points marked with ◊ in figure 5 represent values for the relative deviation of the compared Nusselt numbers for U- and I-fin geometry with average reference temperatures.

As expected, the heat transfer coefficient declines with increasing fin height and fin pitch. Especially, considering the equation from Escoa, the fin height does not influence the overall heat transfer strongly. But with an increasing fin height, the total outside heating surface increases. There could be a gain from the heating surface, for increasing h. The volumetric heat capacity of the heat exchanger with the U-finned tube bundle of the same longitudinal and transverse pitch, same number of tubes, smaller fin pitch, and greater fin height is improved, compared to the I-finned bundle at the same installation size, but greater fin pitch (number of fins per meter). A literature study shows higher effect in heat transfer for a variation of the fin height, see [8]. The most formulas therein are developed for solid fin-tubes. Only the formulas from Escoa and Nir [5] are valid for serrated finned-tubes, as well. A comparison of them shows similar characteristics as seen in [8]. The maximum fin height and the minimum fin pitch result from limitations by finned tube production, as the need to avoid fouling with respect to the kind of fuel (liquid, solid or gaseous).

5.2 Pressure Drop Coefficient Correlations

The pressure drop coefficient correlation of Escoa for "spiro gills" is defined by

$$\xi = 4\left(\frac{d_a + 2h}{d_a}\right)^{1/2} C_2 C_4 C_6 \qquad (20)$$

where

$$C_2 = \left(0.07 + 8\,\mathrm{Re}^{(-0.45)}\right) \qquad (21)$$

$$C_4 = 0.11\left(0.05\frac{t_q}{d_a}\right)^{-0.7\left(\frac{h}{t-s}\right)^{0.23}} \qquad (22)$$

$$C_6 = 1.1 + \left(1.8 - 2.1e^{-0.15N_R^2}\right)\cdot e^{-2\frac{t_l}{t_q}} - \left(0.7 - 0.8e^{-0.15N_R^2}\right)\cdot e^{-0.6\frac{t_l}{t_q}} \qquad (23)$$

A comparison of the two geometries of the heat exchanger is only possible at the same conditions. For ξ_c, the equation

$$\xi_c = \xi_U \left(\frac{d_a + 2h_I}{d_a + 2h_U}\right)^{1/2} \frac{C_{4I}}{C_{4U}} \qquad (24)$$

is obtained. In figure 6, the pressure drop coefficient for eight tube rows in staggered arrangement is shown. The index of ξ indicates the position of the measurement. ξ_1 (zeta1) is calculated from the static pressure differences of the air-side at the finned-tube bundle wall, where ξ_2 (zeta2) is calculated from total pressure differences in the center of the channel. Any flow separation and bypass flow could not be

detected. For Re > 10000 the pressure drop coefficient of the two finned-tube bundles has the same characteristics while for Re < 10000 the small pressure difference of I-shaped finned-tubes shows high uncertainty.

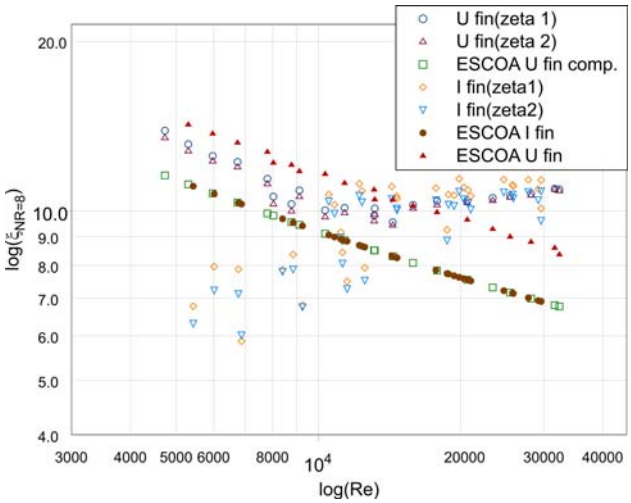

Fig.6: Pressure drop coefficient for 8 tube rows

The U-fin tubes have the same gradient as the Escoa correlation for Re < 15000. For Re ≥ 15000, a small increase takes place, then, at 25000 < Re < 35000 the pressure drop coefficient tends to show a constant value. The pressure drop of the test tubes is higher for the measured *Re*-range than at equation (20). ξ have same values for 8000 < Re < 10000 approximately. The influence of the fin height on the pressure drop at the same installation size indicates an increase of the pressure drop coefficient with h, according to all relations in [8]. This is due to smaller net free area in a tube row, which influences w_E in equation (11) and the pressure drop in equation (10).

5.3 Lévêque-Analogy for Finned-Tubes

An analogy exists between pressure drop and heat transfer for tube bundles based on the "generalized Lévêque-equation", [13]. To calculate heat transfer in case of known pressure drop, the equation writes as follows

$$\frac{Nu}{Pr^{1/3}} = 0.404 \cdot \left(x_f \xi_{1R} \, Re_h^{\,2} \frac{d_h}{L} \right)^{1/3}, \qquad (25)$$

where $x_f = 0.46$ is a factor according to [13], ξ_{1R} the pressure drop coefficient for a single tube row, d_h is the hydraulic diameter ($d_h = 4A/U$), and L is the diagonal pitch of the longitudinal and transverse pitch for staggered arrangement. For more details see [13]. The use of this criterion qualifies the uncertainty of the pressure drop measurement with the help of a comparison of the heat transfer calculation and the "Lévêque-equation".

Figure 7 shows the characteristics for I- and U finned-tube bundles, based on ξ_1 and ξ_2. A comparison with the calculated heat transfer correlation in figure 4 shows good correlation.

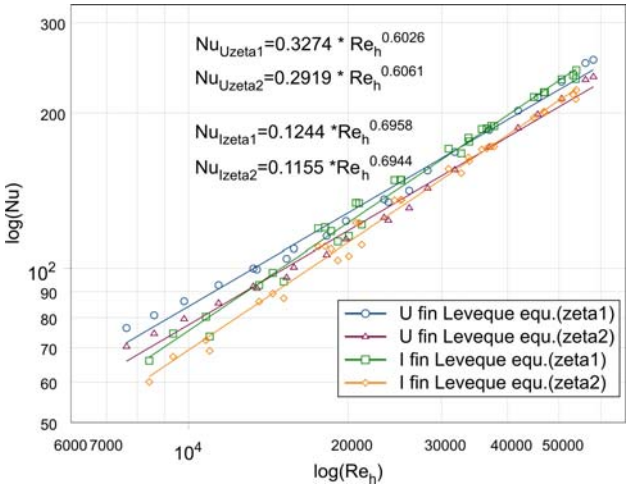

Fig.7: Lévêque-equations according to [13]

The exponents of U-finned tubes are almost the same, where differences between the exponents of the calculated heat transfer correlations and the Lévêque-equations of I-finned tubes could be identified in the uncertainty of the pressure difference measurement for Re < 10000. This underestimates heat transfer for Re < 10000. All pressure drop measurements were carried out at augmented temperatures. As seen by a comparison of figures 4 and 7 there is a good agreement for the prediction of heat transfer correlations, according to the Lévêque-equation. This criterion seems to be valid for finned-tube bundles as well. This indicates a low uncertainty in pressure drop measurement for our arrangement.

6 Performance Comparison of I- and U-Shaped Finned-Tubes

For the evaluation of the performance of a heat exchanger the suggested and developed criterion for single-phase flow from Webb [14] was used.

$$\frac{(\alpha_s A_s)/(\alpha A)}{(P_s/P)^{1/3}/(A_s/A)^{2/3}} = \frac{j_s/j}{(\xi_s/\xi)^{1/3}} = \frac{\left(St_s \, Pr_s^{2/3}\right)/\left(St \, Pr^{2/3}\right)}{(\xi_s/\xi)^{1/3}} \qquad (20)$$

The terms on the left side of this equation $(\alpha_s A_s)/(\alpha A)$, $(P_s/P)^{1/3}$ and $(A_s/A)^{1/3}$ are part of the Colburn-factor ratio for heat transfer and the pressure drop ratio, whereby

$$St = \frac{Nu}{Re \, Pr} = \frac{\alpha}{\rho_{gm} c_{p_{gm}} w_{gm}}. \qquad (21)$$

Heat transfer enhancement using finned-tubes is only achieved by an increase of pressure drop. There are

three different possibilities which are quantified with this criterion: (I) $(\alpha_s A_s)/(\alpha A)$…maximizing the heat transfer rate for equal P_s/P and A_s/A; (II) P_s/P…minimizing the pumping power for equal $(\alpha_s A_s)/(\alpha A)$ and A_s/A; (III) A_s/A …minimizing the overall heat exchanger size for equal P_s/P and $(\alpha_s A_s)/(\alpha A)$. An increase of the heat transfer surface area at the same installation size is only achieved with increasing heat transfer rate at the expense of increasing pressure drop. To optimize the heat exchanger with the help of the performance criterion means to maximize the heat transfer rate with the simultaneous minimization of the pressure drop and the heat exchanger size. As represented in figure 8, the heat transfer rate for I-shaped fins tends to increase for Re < 10000 and Re > 20000. This effect is higher for low Re-numbers. Between 10000 < Re < 20000, no significant difference can be identified. Similar is valid in case of equal α and A, figure 9.

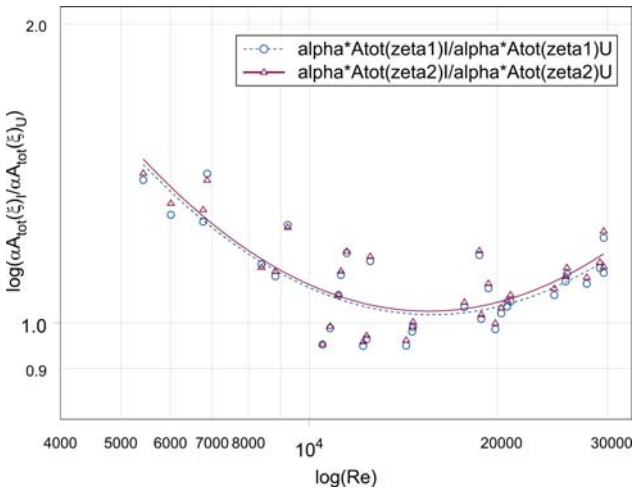

Fig.8: $(\alpha_s A_s)/(\alpha A)$ for equal P_s/P and A_s/A

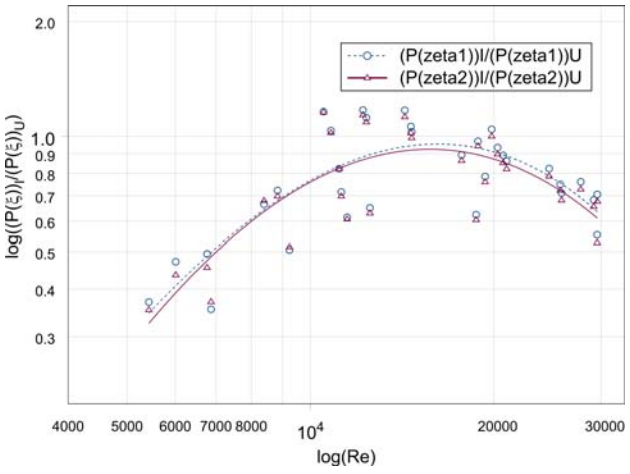

Fig.9: P_s/P for equal $(\alpha_s A_s)/(\alpha A)$ and A_s/A

The pumping power for the I-finned tubes is smaller for Re < 10000 and Re > 20000. In the range of 10000 < Re < 20000 the pumping power shows the same performance. The difference of about 3.36 % of the net free area in a tube row for this two tube geometries was neglected, because of the small calculation error. In figure 10, the ratio of the total outside surface area of the bundles is represented. The α values for the two heat exchangers have only a small variation. To enhance heat transfer, it is necessary to enlarge the tube surface area and/or improve heat conduction.

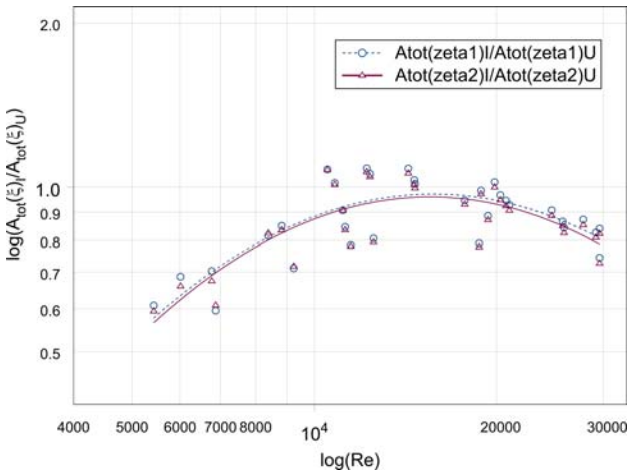

Fig.10: A_s/A for equal P_s/P and $(\alpha_s A_s)/(\alpha A)$

For Re < 10000 and Re > 20000 the installation size of the heat exchanger with U-fins is improved. In the range of 10000 < Re < 20000 no improvement of the heat exchanger size is possible. In figure 11, the ratio of Nusselt numbers for the test tubes is shown.

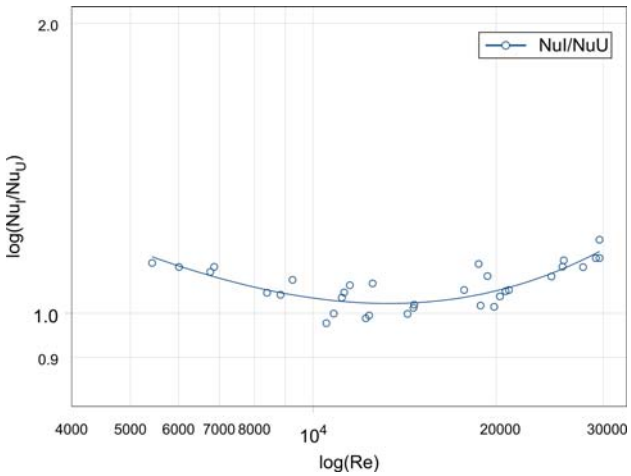

Fig.11: Ratio Nu_I/Nu_U of test tubes

The I-shaped finned tubes tend to improve heat transfer for Re < 10000 and Re > 20000. This relation does not consider the different heat conduction for the U- and I-fin. In the range between 10000 < Re < 20000 the heat exchangers are almost similar, this is the field where no advantage of the pumping power and the heat exchanger surface area could be investigated.

7 Conclusion

Experimental studies have been accomplished in order to be able to compare heat transfer and pressure drop correlations for serrated finned-tubes as well as influences of different geometry parameters e.g. fin height on the performance. After an analysis and evaluation of the measured values, heat transfer and pressure drop correlations have been obtained. A comparison with some correlations from the literature show good congruence with small uncertainty. A performance criterion was applied to characterize the efficiency of the different finned-tube bundles. Three areas, $Re < 10000$, $10000 < Re < 20000$, and $Re > 20000$, of performance evaluation could be identified. Despite the varying fin height and fin pitch of the two different geometries, no substantial difference tendencies could be observed with these equations. An comparison with the Lévêque-equation shows good prediction for the Nusselt number for given pressure drop values. As a next step, further studies of fin tube parameters will be carried out, to clarify the influence of the difference of the fin pitch in the correlations for solid and serrated finned-tubes.

8 Nomenclature

A	surface area	[m²]
A_{fin}	fin surface area of the bundle	[m²]
A_{tube}	bare tube surface area of the bundle	[m²]
A_{tot}	total outside surface bundle-area	[m²]
c_p	specific heat capacity	[J/kgK]
d_a	bare tube diameter	[m]
D_H	hydraulic diameter	[m]
f_a	geometry factor	[-]
F_{min}	net free area in a tube row	[m²]
h	average fin height	[m]
h	specific enthalpy	[J/kg]
k	heat transfer coefficient	[W/m²K]
L	diagonal pitch	[m]
$\dot{m}$	mass flow	[kg/s]
N_R	no. of tubes in the flow-direction	[-]
p	pressure	[N/m²]
Δp	pressure drop	[N/m²]
$\dot{Q}$	heat transfer rate	[W]
s	average fin thickness	[m]
t	fin pitch	[m]
t_l	longitudinal tube pitch	[m]
t_q	transverse tube pitch	[m]
T	temperature	[K]
ΔT_{ln}	log. mean temperature difference	[K]
T_s	average fin temperature	[K]
U	circumference	[m]
$\dot{V}$	volume-flow	[m³/h]
w_E	velocity in the net free area of a row	[m/s]
w_w	velocity of water	[m/s]
x_F	factor according to [13]	[-]
α	heat transfer coefficient	[W/m²K]
η_r	fin efficiency	[-]
λ_r	thermal conductivity of fin	[W/mK]
λ	thermal conductivity	[W/mK]
ρ	density	[kg/m³]
ξ	pressure drop coefficient	[-]
j	Colburn factor	[-]
Nu	Nusselt number	[-]
Pr	Prandtl number	[-]
Re	Reynolds number	[-]
St	Stanton number	[-]

Indices

0	characteristic length at d_a
1, 2	inlet, outlet
8R, 1R	8 tube rows, single tube row
a	outside
b	calculation condition
c	converted
ch	channel
f	fix
g	gas
h	hydraulic
i	inside
I, U	shape of finned-tube
m	average mean
min	minimum
s	I serrated tube
tot	total
w	water

References:

[1] D.R. Reid, J. Taborek, Selection criteria for plain and segmented finned tubes for heat recovery systems , *Transactions of the ASME*, Vol.116, 1994, pp. 406-410.

[2] C. Weierman, Correlations ease the selection of finned tubes, *The Oil and Gas Journal*, Vol.74, No.36, 1976, pp. 94-100.

[3] C. Weierman, J. Taborek, W.J. Marner, Comparison of the performance of in-line and staggered banks of tubes with segmented fins, *The American Institute of Chem. Engineers*, Vol.74, No.174, 1978, pp. 39-46.

[4] S.P. Kearney, A.M. Jacobi, Local convective behavior and fin efficiency in shallow banks of in-line and staggered, annularly finned tubes, *Journal of Heat Transfer*, Vol.118, 1996, pp. 317-325.

[5] A. Nir, Heat transfer and friction factor correlations for cross flow over staggered finned tube banks, *Heat Transfer Eng.*, Vol.12, No.1, 1991, pp. 43-58.

[6] F. Frasz, Waermeuebertragung in Rippenrohr-waermeaustauschern, *Waermeaustauscher,*

Energieeinsparung durch Optimierung von Waermeprozessen, Vulkan-Verlag Essen 2, 1994, pp. 70-76.

[7] K. Kawaguchi, Heat transfer and pressure drop characteristics of finned tube banks in forced convection, *Journal of Enhanced Heat Transfer*, Vol.12, No.1, 2005, pp. 1-20.

[8] F. Frasz, *Berechnung und Auslegung von Rippenrohrwaermeaustauschern*, Fortschritt-Berichte VDI, Reihe 19, No.150

[9] H. Walczyk et al, An experimental study of convective heat transfer from extruded type helical finned tubes, *Chemical Engineering and Processing*, Vol.42, 2003, pp. 29-38.

[10] F. Halici, I. Taymaz, Experimental study of the airside performance of tube row spacing in finned tube heat exchangers, *Heat and Mass Transfer*, Vol.42, 2006, pp. 817-822.

[11] E. Næss, Heat transfer and pressure drop in serrated-fin tube bundles for waste heat recovery applications, *6th World Conference on Experimental Heat Transfer, Fluid Mechanic, and Thermo-dynamics*, 2005, Japan, No.1-a-14, pp.1-5.

[12] K. Hashizume et al, Fin efficiency of serrated fins, *Heat Transfer Engineering*, Vol.23, 2002, pp. 6-14.

[13] H. Martin, V. Gnielinski, Calculation of heat transfer from pressure drop in tube bundles, *3rd European Thermal Sc. Conf. 2000*, pp. 1155-1160.

[14] R.L. Webb, *Principles of enhanced heat transfer*, John, Wiley&Sons, 1994.

[15] ESCOA Turb-X HF Rating Instructions, ESCOA, Pryor, Oklahoma, 1979.

[16] K. Stephan, J. Mitrović, Massnahmen zur Intensivierung des Waermeuebergangs, *Chemie Ingenieur Technik*, 56, Nr.6, 1984, pp. 427-431.

[17] P.K. Konakov, Eine neue Formel fuer den Reibungskoeffizienten glatter Rohre, *Bericht der Akkademie der Wissenschaften der UDSSR*, Vol. 51, Nr.7, 1954, pp. 503-506.